Title

Comparison of Chlorantraniliprole and Flubendiamide Activity Toward Wild-Type and Malignant Hyperthermia-Susceptible Ryanodine Receptors and Heat Stress Intolerance

Journal

Toxicological Sciences, 167(2)

ISSN

1096-6080

Authors

Truong, Kim M
Pessah, Isaac N

Publication Date

2019-02-01

DOI

10.1093/toxsci/kfy256

Peer reviewed

OXFORD

SOT | Society of Toxicology
www.toxsci.oxfordjournals.org

TOXICOLOGICAL SCIENCES, 2018, 1–15

doi: 10.1093/toxsci/kfy256
Advance Access Publication Date: October 17, 2018
Research Article

Comparison of Chlorantraniliprole and Flubendiamide Activity Toward Wild-Type and Malignant Hyperthermia-Susceptible Ryanodine Receptors and Heat Stress Intolerance

Kim M. Truong and Isaac N. Pessah[1]

Department of Molecular Biosciences, School of Veterinary Medicine, University of California, Davis, California 95616-5270

[1]To whom correspondence should be addressed at 1089 Veterinary Medicine Drive, Davis, CA 95616. Fax: +1-(530)-752-4698. E-mail: inpessah@ucdavis.edu.

ABSTRACT

Chlorantraniliprole (CP) and flubendiamide (FD) are widely used in agriculture globally to control lepidopteran pests. Both insecticides target ryanodine receptors (RyRs) and promote Ca^{2+} leak from sarcoplasmic reticulum (SR) within insect skeletal muscle yet are purportedly devoid of activity toward mammalian RyR1 and muscle. RyRs are ion channels that regulate intracellular Ca^{2+} release from SR during physiological excitation-contraction coupling. Mutations in *RYR1* genes confer malignant hyperthermia susceptibility (MHS), a potentially lethal pharmacogenetic disorder in humans and animals. Compared with vehicle control, CP (10 μM) triggers a 65-fold higher rate of Ca^{2+} efflux from Ca^{2+}-loaded mammalian WT-RyR1 SR vesicles, whereas FD (10 μM) produces negligible influence on Ca^{2+} leak. We, therefore, compared whether CP or FD differentially influence patterns of high-affinity [^{3}H]ryanodine ([^{3}H]Ry) binding to RyR1 isolated from muscle SR membranes prepared from adult C57BL/6J mice expressing WT, homozygous C-terminal MHS mutation T4826I, or heterozygous N-terminal MHS mutation R163C. Basal [^{3}H]Ry binding differed among genotypes with rank order T4826I ≫R163C∼WT, regardless of [Ca^{2+}] in the assay medium. Both CP and FD (0.01–100 μM) elicited concentration-dependent increase in [^{3}H]Ry binding, although CP showed greater efficacy regardless of genotype or [Ca^{2+}]. Exposure to CP (500 mg/kg; *p.o*) failed to shift intolerance to heat stress (38°C) characteristic of R163C and T4826I MHS mice, nor cause lethality in WT mice. Although nM-μM of either diamide is capable of differentially altering WT and MHS RyR1 conformation *in vitro*, human RyR1 mutations within putative diamide N- and C-terminal interaction domains do not alter heat stress intolerance (HSI) *in vivo*.

Key words: chlorantraniliprole; flubendiamide; diamides; insecticides; ryanodine receptors; malignant hyperthermia.

Anthranilic diamides, including chlorantraniliprole (CP), and phthalic diamides, including flubendiamide (FD), are 2 emerging classes of insecticides used to control lepidopteran agricultural pest damage worldwide (Adams *et al.*, 2016; Cameron *et al.*, 2015). Both classes of diamide insecticides bind to and stimulate the insect ryanodine receptors (RyRs) to disrupt intracellular calcium ($[Ca^{2+}]_i$) homeostasis, leading to muscle paralysis and death (Lahm *et al.*, 2009). RyR1 and RyR2 are homotetrameric Ca^{2+} channels localized on mammalian sarcoplasmic reticulum (SR) of skeletal and cardiac muscle, respectively, but both genetic isoforms are also broadly expressed on the endoplasmic reticulum (ER) of nonmuscle cells (Pessah *et al.*, 2010). RyR channels are not only an essential component of the physiological process of excitation-contraction coupling (EC coupling), loss or gain of RyR channel function are associated with heritable disorders of muscle in humans and animals and have been the subject of several recent reviews (Dulhunty *et al.*, 2017; Meissner, 2017; Riazi *et al.*, 2018; Voermans *et al.*, 2016; Yamada *et al.*, 2017). Although mammals and insects both express RyRs that serve similar physiological roles in $[Ca^{2+}]_i$ maintenance,

diamide insecticides show high selectivity for insect RyRs over mammalian homologs (Casida, 2015; Isaacs *et al.*, 2012; Sattelle *et al.*, 2008; Selby *et al.*, 2013).

Mammals possess 3 RyR isoforms: RyR1, RyR2, and RyR3, which are found predominantly in skeletal, cardiac, and smooth muscle, as well as the central and peripheral nervous systems and the immune system. In contrast, insects solely express 1 RyR isoform (Sattelle *et al.*, 2008; Sun *et al.*, 2016). Insects share >80% RyR amino acid similarity among one another but only ~45% similarity to mammalian RyRs (Kato *et al.*, 2009; Sattelle *et al.*, 2008; Xu *et al.*, 2000). RyR sequence divergence accounts for the great selectivity of diamide insecticides toward insect RyRs over mammalian RyRs, and thus has been posited to be the basis of their large safety margin. Previous research has shown that while CP and FD have distinct binding sites on insect RyR, the 2 binding sites reside near the C-terminus transmembrane region encompassing amino acids 4111–5084, with FD also requiring N-terminal residues 183–290 to exert its activating influences on the channel (Isaacs *et al.*, 2012; Kato *et al.*, 2009; Tao *et al.*, 2013). Strong experimental data have established that the divergent amino acid sequences between wild-type (WT) mammalian RyR1 and insect muscle RyRs in large part accounts for the low potencies of CP and FD toward mammalian skeletal muscle. However, to date, there are no studies investigating whether gain of function mutations near or within the N- or C-regions of RyR1, regions important for insecticidal activity and also known to be expressed in humans with malignant hyperthermia (MH) susceptibility, alter sensitivity to diamide insecticides.

RyR1 mutations that confer malignant hyperthermia susceptibility (MHS) typically cause a gain-of-function Ca^{2+} leak from SR (Lyfenko *et al.*, 2004; Robinson *et al.*, 2006) resulting in chronically elevated cytoplasmic resting $[Ca^{2+}]_i$ (Zhou *et al.*, 2018a). Most MH mutations are transmitted in an autosomal dominant manner with genetic prevalence as high as 1:3000 (Fagerlund *et al.*, 1997; Rosenberg *et al.*, 2007; Wappler, 2010). MHS individuals when exposed to volatile general anesthetics, such as isoflurane or sevoflurane, or to prolonged heat stress, undergo an episode consisting of, but not limited to, rapid onset of metabolic acidosis, skeletal muscle rigidity, elevated core temperature, and if left untreated, death (Kim, 2012; Rosenberg *et al.*, 2007).

An important unanswered question is whether RyR1 mutations residing near or within regions identified as critical for diamide activity in insects and known to confer MHS in humans, influence the potency and/or efficacy of CP or FD toward activation (leakiness) of the mammalian RyR1 channel, and more importantly, whether they enhance susceptibility to heat stress intolerance (HSI) *in vivo*. Therefore, to bridge this gap in knowledge, we prepared muscle SR from WT mice and MHS mice either heterozygous for human N-terminal mutation RyR1-R163C (Feng *et al.*, 2011; Yang *et al.*, 2006) or homozygous for human C-terminal mutation RyR1-T4826I (Barrientos *et al.*, 2012; Yuen *et al.*, 2012) to compare how CP and FD influence Ca^{2+}-dependent [^{3}H]ryanodine ([^{3}H]Ry) binding *in vitro*, and to also assess responses to heat stress *in vivo*.

MATERIALS AND METHODS

Chemicals

CP (≥99.3%) and FD (≥98.3%) were obtained from either AccuStandard (New Haven, Connecticut) or Chem Service Inc. (West Chester, Pennsylvania). [^{3}H]Ryanodine (56.6–111 Ci/mmol) was obtained from Perkin Elmer Life (Bellerica, Massachusetts). Ryanodine (≥98.3%) was obtained from Tocris Bioscience (Minneapolis, Minnesota). Arsenazo III (≥95%) was obtained from Santa Cruz Biotechnology (Dallas, Texas). The following were obtained from Sigma-Aldrich (St. Louis, Missouri): Adenosine 5′-triphosphate magnesium salt (≥95%), phosphocreatine disodium salt hydrate (≥97%), cyclopiazonic acid (≥98%), ruthenium red, type 1 creatine phosphokinase, leupeptin hydrochloride, phenylmethylsulfonyl fluoride, and methyl cellulose viscosity: 4000 cP.

Animals

Collections of mouse and rabbit tissues for the studies were conducted using protocols approved by the Institutional Animal Care and Use Committee (IACUC) at University of California at Davis (UCD; Davis, California). Heat stress procedures performed in studies involving mice were in accordance with the ethical standards of the IACUC at UCD (Davis, California). WT and both MHS heterozygous R163C and homozygous T4826I mice were generated with a knock-in mutation-targeting vector as described previously, and bred into the C57BL/6 background (Yang *et al.*, 2006; Yuen *et al.*, 2012). Mouse genotypes were verified by GenoTyping Center of America (Ellsworth, Maine) through PCR screening. PCR primer sequences were as follows: RyR1-WT (forward), GAG AGA AGG TTC GAG TTG GGG AT; RyR1-WT (reverse), ACT CAC CAG GTA TCG CTC AG; RyR1-R163C (forward), GAG AGA AGG TTT GCG TTG GAG AC; RyR1-R163C (reverse), ACT CAC CAG GTA TCG CTC AG; RyR1-T4826I (forward), GGA CCT CAT TGG CTA CTT CG; RyR1-T4826I (reverse), CTG ACC AGC CAA TCC AAG TT.

Junctional sarcoplasmic reticulum (JSR) membrane preparation from rabbit muscles

To test whether CP or FD trigger Ca^{2+} release from skeletal muscle terminal cisternae, RyR1-enriched JSR membrane fractions were isolated from the back and hind limb skeletal muscles of WT male (1.5 kg) New Zealand White rabbits (Charles River, Hollister, California) as described previously (Pessah *et al.*, 1986; Saito *et al.*, 1984; Zhang and Pessah 2017). Approximately 200 g of tissue was flash frozen in liquid nitrogen and quickly pulverized into a fine powder, which was subsequently homogenized in a Waring blender for 1 min in homogenization buffer (pH 7.4) containing 300 mM sucrose, 5 mM imidazole, 100 μM phenylmethylsulfonyl fluoride (PMSF), and 10 μg/ml leupeptin hydrochloride. The mixture was centrifuged for 10 min at 8100 RPM. Subsequently, the supernatant was removed and the remaining pellet re-homogenized and centrifuged again. Supernatants were combined, and the mixture was filtered through a mesh sieve before centrifuged at *110 000g* for 1 h at 4°C. The pellet was gently rinsed with homogenization buffer, homogenized with a glass Dounce, and transferred to the top of a discontinuous sucrose gradient (45%, 38%, 34%, 32%, and 27%, w/v; dissolved in homogenization buffer). The gradient was centrifuged at 20 000 RPM for 15 h at 4°C. Supernatant from the 38% and 45% fractions were pooled and diluted to 10% sucrose using a 5 mM imidazole solution. The mixture was centrifuged again at *110 000g* for 1 h at 4°C. Final JSR pellets were resuspended in ice-cold buffer (pH 7.4) containing 300 mM sucrose and 10 mM HEPES, aliquoted, flash frozen, and stored at −80°C.

Microsomal preparations of mouse muscles

Skeletal muscle crude membrane microsomal fractions were prepared from 5- to 7-month-old congenic WT C57BL/6J mice, mice heterozygous for a human MHS mutation in the N-terminal of RyR1 (RyR1-R163C), and mice homozygous for a human MHS mutation in the C-terminal region of RyR1 (RyR1-T4826I) as described previously (Barrientos *et al.*, 2012; Feng *et al.*, 2011). Briefly, limb skeletal muscles from each genotype (2–3 male mice/preparation) were flash frozen, pulverized, and placed into ice-cold buffer (pH 7.4) containing (in mM) 300 sucrose, 10 HEPES, 10 μg/ml leupeptin hydrochloride, 0.1 phenylmethylsulfonyl fluoride (PMSF), 10 sodium fluoride, 2 β-glycerophosphate, 0.5 sodium orthovanadate, and 1.5 ethylene glycol tetraacetic acid (EGTA). A PowerGen 700 D (Fisher Scientific, Waltham, Massachusetts) was used to homogenize the suspension with 3 sequential bursts of 30 s at 10 000 RPM. Homogenates were centrifuged at 1000 RPM for 1 min and the supernatant poured through a mesh sieve to remove large components. The collected supernatants were centrifuged at *110 000g* for 60 min at 4°C. Final pellets were resuspended in ice-cold buffer (pH 7.4) containing 300 mM sucrose and 10 mM HEPES, aliquoted, flash frozen, and stored at −80°C.

Protein concentration determination

All membrane protein preparation concentrations were determined using the Pierce BCA protein assay kit (Thermo Fisher, Waltham, Massachusetts).

Assessment of macroscopic Ca^{2+} fluxes across JSR membrane vesicles

Metallochromic Ca^{2+} indicator dye arsenazo III was used to measure net Ca^{2+} uptake and efflux across JSR membrane vesicles in real-time as described previously with antipyrylazo III (Niknam *et al.*, 2013; Pessah *et al.*, 2006; 2009). JSR membrane vesicles (100 μg/ml) were placed in cuvettes at 35°C with medium (pH 7.4) consisting of (in mM) 100 KCl, 6 sodium pyrophosphate, 0.25 arsenazo III (AIII), and 20 4-morpholinepropanesulfonic acid (MOPS), 2 Mg^{2+}ATP, 10 phosphocreatine, and 20 μg/ml creatine phosphokinase (used as coupling enzyme). Ca^{2+} loading was accomplished by 3 sequential additions of $CaCl_2$ totaling 45 nmol. Once JSR vesicles were loaded with Ca^{2+} to near their capacity, they were exposed to 0.1% DMSO (v/v) vehicle control, 10 μM CP, or 10 μM FD to determine their ability to mobilize Ca^{2+} accumulated in the vesicle (ie, trigger Ca^{2+} leak). In some experiments, 2 μM ruthenium red was added once Ca^{2+} leak was observed to completely block RyR1, followed by 50 μM cyclopiazonic acid to completely inhibit active pumping by SERCA (SR/ER Ca^{2+}-ATPase). AIII signals were calibrated at the end of each experiment by stepwise addition of $CaCl_2$ from a National Bureau of Standard stock.

[^{3}H]Ryanodine ([^{3}H]Ry) binding analysis

Specific [^{3}H]Ry binding to mouse skeletal muscle RyR1 microsomes in suboptimal (1 μM), optimal (50 μM), and inhibitory (1 mM) Ca^{2+} concentrations ([Ca^{2+}]) was measured as established previously (Pessah and Zimanyi 1991; Pessah *et al.*, 1985). Each experiment was performed in triplicate ($n = 3$) and replicated twice. Skeletal microsomes (100 μg/ml) were incubated with ice-cold binding buffer (pH 7.4) composed of (in mM) 250 KCl, 15 NaCl, and 20 HEPES, with Ca^{2+} buffered to a concentration of 1 μM, 50 μM, or 1 mM for binding of 5 nM [^{3}H]Ry under equilibrium assay conditions (3 h; 37°C). Assays were performed in the absence or presence of increasing concentration of CP or FD (0.01–100 μM) with constant shaking. Bound and Determined (BAD) program was used to calculate the concentration of ethylene glycol-bis(2-aminoethylether)-*N*, *N*, *N*′, *N*′-tetraacetic acid (EGTA) necessary to achieve the desired free [Ca^{2+}] (Brooks and Storey, 1992). Non-specific binding was determined by incubating with 1000-fold (5 μM) excess of unlabeled ryanodine in the absence or presence of specified compound. Bound from free ligand was separated by filtration through Whatman GF/B glass fiber filters (Whatman, Clifton, New Jersey) using a cell harvester (Brandel, Gaithersburg, Maryland) and washed thrice with 5 mL of ice-cold harvesting buffer (pH 7.4) consisting of (in mM) 140 KCl, 0.1 $CaCl_2$, and 10 HEPES. Filters were completely submerged in 4 mL of scintillation fluid (ScintiVerse BD Cocktail, Fisher Scientific, Waltham, Massachusetts) and [^{3}H]Ry trapped to the filter quantified using a Beckman Coulter LS6500 spectrometer (Beckman Coulter, Indianapolis, Indiana). Each experiment was performed in triplicates ($n = 3$) and replicated using different membrane preparations with final DMSO concentration ≤1% (v/v).

Study of heat stress intolerance (HSI)

HSI tests were performed on 6- to 10-month-old (30–50 g) male C57BL/6J WT mice ($n = 5$), R163C heterozygous mice ($n = 6$), or T4826I homozygous mice ($n = 6$). Mice from each genotype were randomly assigned to 2 treatment groups: 0.5% aqueous methyl cellulose vehicle control or 500 mg/kg bw CP (50 mg/ml). At 5 AM all mice were dosed by oral gavage (18G x 1.5″, 2 mm flex polytetrafluoroethylene with metal bite protector [Cadence Science, Cranston, Rhod Island]) since *p.o.* is recognized as the most efficient method of entry for CP (Bentley *et al.*, 2010b). Although absorption of CP is incomplete and dose related, we proceeded with a high-dose oral exposure protocol established by Dupont (FAO/WHO, 2008). A high dose was chosen because: (i) CP does not readily go into solution in aqueous methyl cellulose, and (ii) it permits a small volume of CP by gavage, minimizing potential variability in the actual CP dose administered. Post dosing, the mice were permitted to freely roam in their respective home cages with food and water *ad libitum* for 12 h (T_{max}) to achieve C_{max} (5.1 μg/g) (Bentley *et al.*, 2010b; FAO/WHO, 2008; Himmelstein, 2006a; Wolterink, 2008) to ensure CP broadly distributes to organs, including highly perfused skeletal muscle compartments. At 5 PM, a rectal probe was inserted in each mouse to measure and continuously record core temperature. They were then restrained in medium mouse holders (Kent Scientific Corp., Torrington, Connecticut) to acclimate for 5 min at room temperature before initiating the heat stress protocol in a 38°C incubator. Heat stress was terminated after 60 min or earlier if the mouse underwent a fulminant MH episode and died. Core body temperature for the duration of the study was recorded by the Temperature Controller 324B and CL-100 from Warner Instrument, which was connected with the digitizer from Axon Instruments Digitizer 1320A at a sampling rate of 1 Hz by AxoScope software (V.9.0; Molecular Devices, Sunnyvale, California).

Statistical analysis

GraphPad Prism 7 software (La Jolla, California) was used to make comparisons using a one-way ANOVA with either a Tukey's *post hoc* test or a Dunnett's *post hoc* test, or a Student's *t*-test, where appropriate (*$p < .05$; **$p < .01$; ***$p < .001$). GraphPad Prism 7 was also used to generate linear regression traces to

determine Ca^{2+} release rate, and for nonlinear curve fitting to determine EC_{50} values and maximum response. Survival curves were compared with a log-rank (Mantel-Cox) analysis (*$p < .03$; **$p < .002$; ***$p < .0002$). All error bars represent standard error of the mean (SEM). Statistical analyses used for each data set are given in their respective figure legends.

RESULTS

CP, But Not FD, Triggers Ca^{2+} Leak from Mammalian JSR in the Presence of Sarco-Endoplasmic Reticulum Ca^{2+}-ATPase (SERCA) Activity

It is firmly established that both CP and FD directly activate *Lepidoptera* RyR by interacting with critical amino acids within the C-terminal transmembrane assembly (Figs. 1A–C) (Lahm *et al.*, 2009; Sattelle *et al.*, 2008). Whether either insecticide can elicit an RyR1-mediated Ca^{2+} leak from adult mammalian JSR has not yet been adequately addressed. Therefore, we utilized a well-established macroscopic Ca^{2+} transport assay consisting of enriched RyR1-JSR vesicles and the Ca^{2+}-sensitive dye AIII to determine whether: (i) either/or both insecticides mediate efflux from SR stores, and (ii) whether any Ca^{2+} leak observed was mediated by interaction with RyR1. Three sequential addition of $CaCl_2$ resulted in active Ca^{2+} accumulation into the JSR lumen through sarco/endoplasmic Ca^{2+}-ATPase (SERCA) pump activity (Figure 2A). Once extravesicular [Ca^{2+}] returned to baseline, subsequent addition of DMSO control did not alter baseline leak rate, consistent with previous reports (Feng *et al.*, 2017; Niknam *et al.*, 2013). Addition of low (nM) concentrations of CP or FD also failed to elicit net Ca^{2+} efflux from the JSR vesicles (not shown). However, a higher concentration of CP (10 μM) elicited net efflux of luminal Ca^{2+} from JSR vesicles with an initial rate 65-fold greater than baseline leak rate measured from DMSO control (Figs. 2B and 2C). In sharp contrast, FD (10 μM) failed to elicit a net Ca^{2+} leak significantly different from DMSO control (Figs. 2B and 2C). Once the CP-triggered Ca^{2+} leak was initiated, subsequent addition of RyR1 channel blocker ruthenium red caused rapid SERCA-dependent Ca^{2+} reaccumulation into the JSR vesicles, indicating CP-triggered Ca^{2+} efflux was mediated by selective influences on RyR1 channels without appreciable impact on SERCA pumps. In support of this interpretation, addition of SERCA inhibitor cyclopiazonic acid caused complete release of luminal JSR Ca^{2+} from all treatment groups (Figure 2A).

CP and FD Differentially Influence [^{3}H]Ry Binding from WT and MHS RyR1

Nanomolar [^{3}H]Ry is used as a specific probe that binds to the open state of RyRs; due to its sensitivity to RyR conformational changes, it is widely used to quantitatively investigate the effect, positive or negative, mediated by a compound through RyR allosteric modulation (Hawkes *et al.*, 1992; Isaacs *et al.*, 2012; Niknam *et al.*, 2013; Pessah and Zimanyi 1991; Pessah *et al.*, 1987). Basal level [^{3}H]Ry bound was highly dependent on free [Ca^{2+}] in the assay medium as well as the genotype of the animals from which microsomes were prepared (Figure 3). RyR1-T4826I preparations showed the highest levels of [^{3}H]Ry binding at each of the 3 free [Ca^{2+}] tested, but maintained the expected bell-shaped relationship with respect to suboptimal (1 μM), optimal (50 μM), and inhibitory (1 mM) Ca^{2+} (Barrientos *et al.*, 2012). However, unlike RyR1-WT and RyR1-R163C preparations that were almost completely inhibited in the presence of 1 mM Ca^{2+}, RyR1-T4826I maintained appreciable [^{3}H]Ry occupancy (Figure 3). While a significant difference in [^{3}H]Ry binding between RyR1-WT and RyR1-R163C at suboptimal 1 μM Ca^{2+} and optimal 50 μM Ca^{2+} is observed with low [^{3}H]Ry (2 nM) (Feng *et al.*, 2011), increasing [^{3}H]Ry 2.5-fold higher (5 nM) mitigates resolution of significant differences, although the same trend remains: [^{3}H]Ry binding for RyR1-R163C>RyR1-WT (Figure 3).

CP and FD (≥1μM) produced a concentration-dependent increase in [^{3}H]Ry binding in all 3 genotypes (Figs. 4–6). RyR1-WT and MHS RyR1 preparations generally showed EC_{50} values for CP insignificantly different from each other, except in the presence of suboptimal 1 μM Ca^{2+} where CP showed 2–4-fold lower apparent potency toward RyR1-WT (Figs. 4A, 4C, and 4E). FD only showed significantly higher potency toward RyR1-T4826I when measured in the presence of inhibitory 1 mM Ca^{2+} (Figs. 6B, 6D, and 6E). It must be noted, however, that the relative enhancement of [^{3}H]Ry binding elicited by CP or FD was highly dependent on genotype, and directly influenced by the level of baseline binding characteristic of each genotype at each [Ca^{2+}] tested (Figure 3). Comparisons of CP and FD concentration-effect relationships among genotype are presented individually for each [Ca^{2+}] assayed.

Suboptimal 1 μM Ca^{2+}

Although CP at maximum concentration (100 μM) produced similar maximum levels of [^{3}H]Ry binding for all 3 genotypes (Figure 4A), relative to their respective baseline, CP showed a ranked efficacy of RyR1-WT≫RyR1-R163C>RyR1-T4826I (Figs. 4C and 4E). FD showed weaker percent enhancement relative to respective baselines than CP with RyR1-WT and RyR1-R163C (FD producing 23%–24% change from baseline binding compared with CP) (Figs. 4C–E). RyR1-T4826I showed similar relative efficacies with FD achieving 87% of the baseline increase observed with CP, but this was mainly due to the significantly higher baseline of RyR1-T4826I in the absence of either insecticide (Figs. 4A, 4B, and 4E). EC_{50} values for all 3 genotypes also showed an inverse relationship where potency was highest with RyR1-T4826I and lowest with RyR1-WT (Figure 4E). The lowest observed effective concentration (LOEC)—the lowest concentration that elicits a statistically significant increase in [^{3}H]Ry binding compared to DMSO control—were identical between RyR1-WT and RyR1-R163C for both insecticides. However, and possibly biologically significant, the RyR1-T4826I LOEC was observed at a >100-fold lower concentration where 10 nM of FD or CP significantly ($p < .01$) increased [^{3}H]Ry binding 2–2.5-fold compared to vehicle control.

Optimal 50 μM Ca^{2+}

In the presence of optimal Ca^{2+} the RyR1 channel open conformation is facilitated and increases [^{3}H]Ry binding to high affinity sites (Pessah *et al.*, 1985, 1987). Under these assay conditions, RyR1-T4826I channels are nearly maximally bound with [^{3}H]Ry, thus neither CP nor FD, even at a very high concentration (100 μM), are capable of additional enhancement of [^{3}H]Ry binding (Figs. 5A–E). While there was no significant difference in diamide insecticide potency (EC_{50}) regardless of genotype, the maximum response relative to respective baseline binding differed significantly among the genotypes (Figure 5E). In contrast to comparisons of relative efficacy observed in the presence of suboptimal Ca^{2+}, FD was only slightly less efficacious than CP (75%–78%) toward RyR1-WT and RyR1-R163C, but not different toward RyR1-T4826I (96%) likely due to complete saturation of binding sites achieved in the presence of optimal Ca^{2+} alone

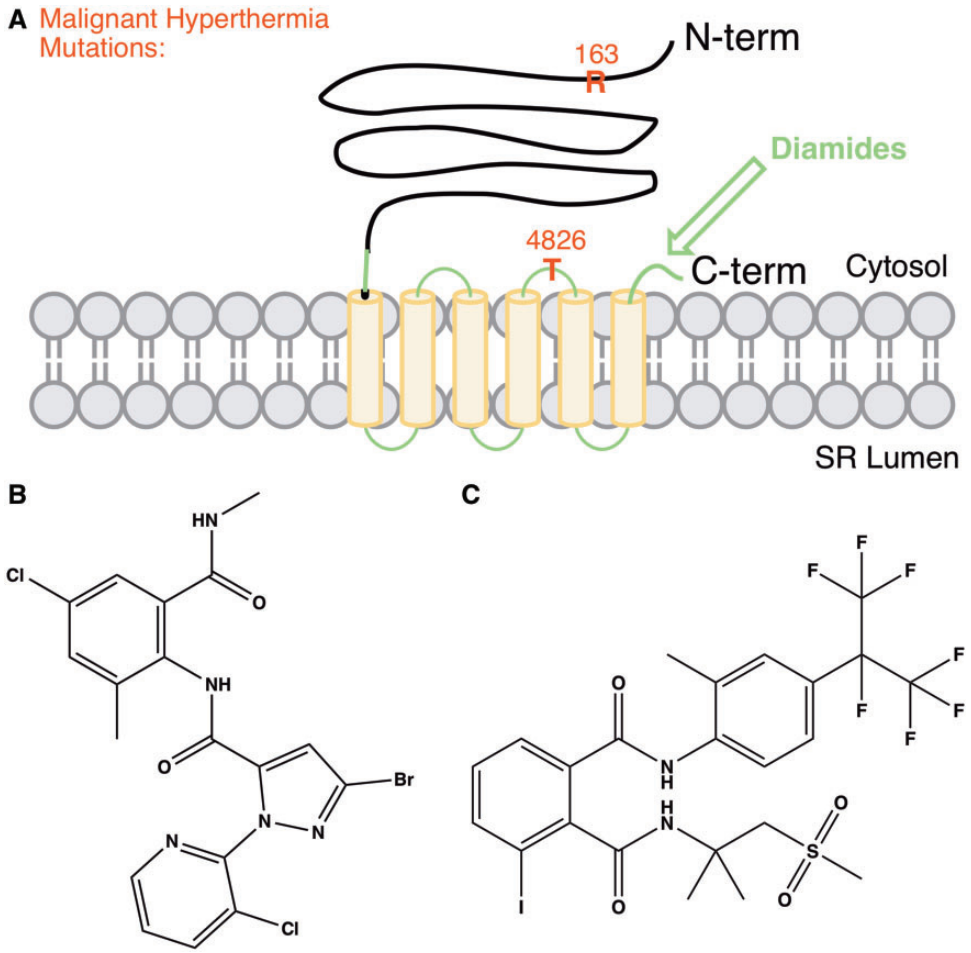

Figure 1. (A) RyR type 1 (RyR1) MH mutations in humans may confer sensitivity to the activating effects of insecticides (B) anthranilic diamide CP and/or (C) phthalic diamide FD. In insects, the diamides bind near the C-terminus or transmembrane domain (amino acids 4111–5084) of the RyR to cause muscle paralysis, and ultimately death.

(Figs. 5A–E). Similar to suboptimal Ca^{2+}, LOEC were identical between RyR1-WT and RyR1-R163C for both diamide insecticides.

Inhibitory 1 mM Ca^{2+}

Millimolar Ca^{2+} promotes a closed RyR1 channel confirmation that decreases [^{3}H]Ry binding to high-affinity sites (Ma *et al.*, 1988; Meissner 1994; Pessah and Zimanyi 1991). As expected, 1 mM Ca^{2+} reduced baseline [^{3}H]Ry binding with both RyR1-WT and RyR1-R163C, but not with RyR1-T4826I where baseline binding levels were similar to suboptimal to optimal Ca^{2+} concentrations (Figure 3). CP (>1 μM) significantly increased [^{3}H]Ry binding for all 3 genotypes (Figs. 6A, 6C, and 6E), although such effects were modest with RyR1-T4826I. FD (>1 μM) significantly increased [^{3}H]Ry binding for RyR1-WT and RyR1-R163C, but not RyR1-T4826I (Figs. 6B, 6D, and 6E). The range by which FD increased [^{3}H]Ry binding was 4- to 6-fold lower than CP (Figure 6E). These data suggest that CP was more effective than FD at overriding the inhibitory effect of 1 mM Ca^{2+} across all 3 genotypes.

CP Does Not Influence Heat Stress Intolerance (HSI) in MHS Mice

Mice expressing human RyR1 MHS mutations are well-known to be heat stress intolerant (HSI) and undergo a fulminant episode characterized by rapid elevation of core temperature and death (Chelu *et al.*, 2006; Yang *et al.*, 2006; Yuen *et al.*, 2012). Since FD has been withdrawn from use in the United States due to its toxic metabolites (EPA 2018), we proceeded with CP to determine whether it influences core body temperature during moderate heat stress of mice expressing either WT, heterozygous R163C (R163C HET), or homozygous T4826I (T4826I HOM) RyR1. A study by Dupont determined CP plasma half-life to be 43 h with optimal plasma concentration (C_{max}: 5.1 μg/g) at 12 h (T_{max}) post high oral CP dose (Bentley *et al.*, 2010a; FAO/WHO, 2008). Therefore, to mirror the same exposure paradigm as what has already been established, we commenced our heat stress study 12-h post oral dosing to ensure for broad distribution of CP to all organs, including skeletal muscle.

The mice were acclimatized in their respective restrainer 5 min before heat stress. Restrainer-acclimatized mice did not display significantly different core temperatures with respect to genotype or treatment (Figure 7A). Mice were subjected to 38°C for 60 min or until MHS mice exhibited the onset of a fulminant MH episode (limb extension and curved rigid tail) which invariably proved lethal. Mean core temperature recorded at the end of the 60-min heat stress protocol (WT) or at time of triggering fulminant MH (R163C HET and T4826I HOM) were similar regardless of treatment (Figure 7B). In the vehicle control group,

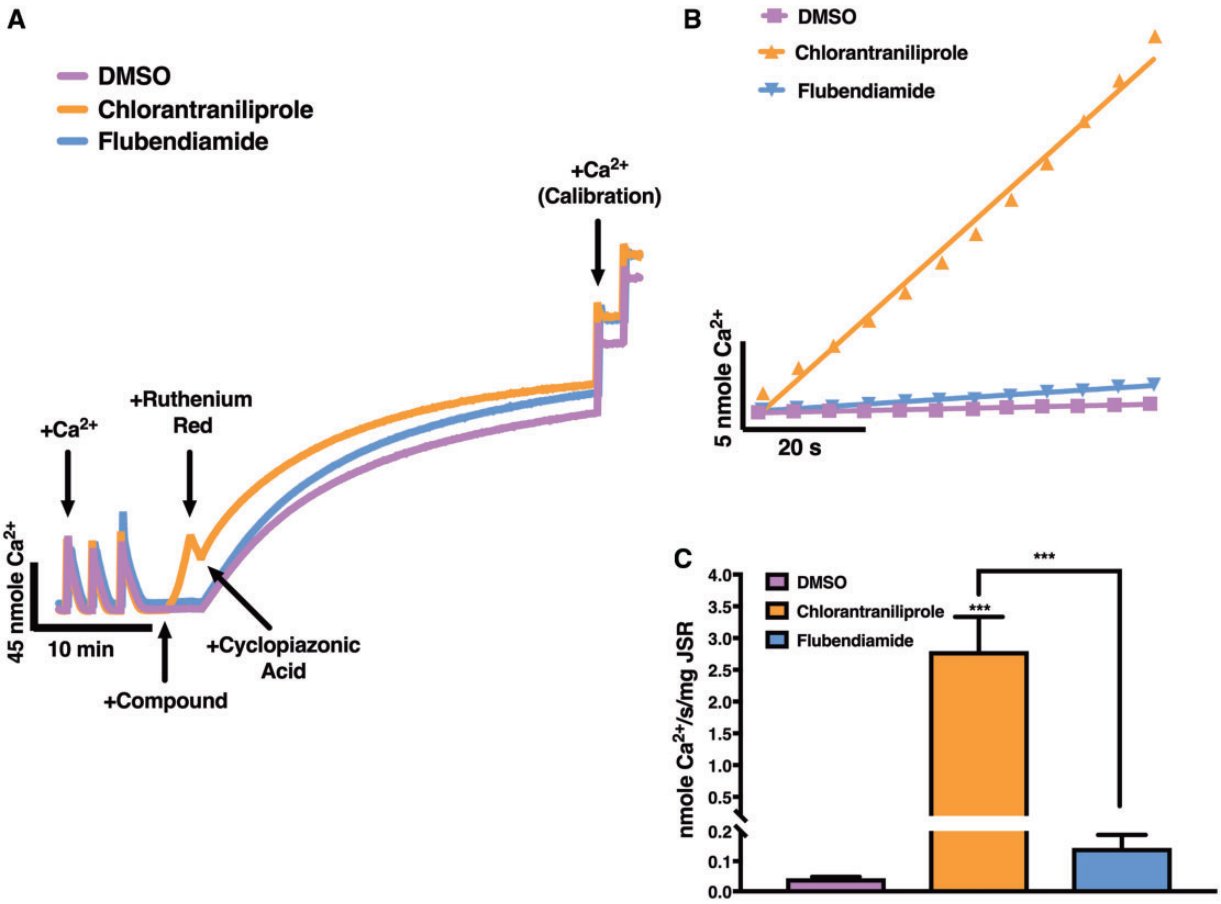

Figure 2. CP and, to a much lesser degree, FD potentiate Ca^{2+} release from SR stores through direct activation of RyR1. (A) Schematic trace detailing the Ca^{2+} efflux assay: JSR vesicles were actively loaded with Ca^{2+} to near maximal capacity and then exposed to either DMSO vehicle control, 10 μM CP, or 10 μM FD to determine compound effect on RyR1 activation. Following, 2 μM ruthenium red, a RyR blocker, was added to determine if Ca^{2+} release mediated by the diamides was induced by direct interaction with RyR1. Lastly, 50 μM cyclopiazonic acid, a sarco/endoplasmic Ca^{2+}-ATPase (SERCA) inhibitor, was added to prevent reuptake of Ca^{2+} to allow for calibration of Ca^{2+}. (B) The initial 60 s of the Ca^{2+} release trace for DMSO vehicle control (square trace), 10 μM CP (triangle trace), and 10 μM FD (inverted triangle trace) was assessed with a linear regression to determine Ca^{2+} release rate (nmole Ca^{2+}/s/mg JSR). (C) CP triggered a 65-fold higher rate of Ca^{2+} efflux from Ca^{2+}-loaded WT-RyR1 SR vesicles compared with baseline leak rate, whereas FD only triggered a 3-fold difference. Three to five independent measurements replicated 3 times ($n = 3$) from different preparations under identical condition were summarized and plotted. Data presented as mean ± SEM (***$p = \leq .001$, one-way ANOVA with Tukey *post hoc* test).

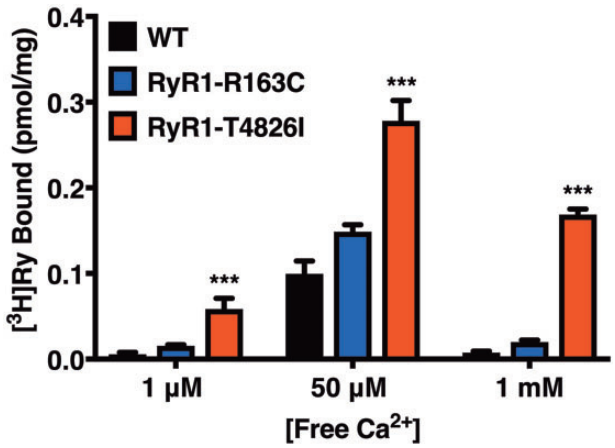

Figure 3. Basal level of [^{3}H]ryanodine ([^{3}H]Ry) bound is highly dependent on both genotype and the free [Ca^{2+}] in the assay medium. A one-way ANOVA with Tukey *post hoc* test confirmed basal [^{3}H]Ry binding with RyR1-T4826I preparations was significantly higher than RyR1-WT or RyR1-R163C at each of the 3 free [Ca^{2+}] tested (***$p < .001$).

the latency time to lethal MH episode was similar for both T4826I HOM and R163C HET mice (7.3 ± 0.4 vs 6.8 ± 0.7 min, respectively), as were their mean terminal core body temperatures (42.1 ± 0.3 vs 42.3 ± 0.6°C, respectively) (Figs. 7B and 7C). At the time MHS mice exhibited the fulminant phenotype, WT mice showed significantly lower core body temperature (40 ± 0.2°C; $p < .01$) (Figs. 7B and 7C). Body temperature of WT mice exposed to prolonged moderate heat stress continued to rise with no ill effects (ie, 100% survival), reaching 41.7 ± 0.2°C at 60 min, which was comparable to MHS mice at time of death (Figs. 7B and 7C). The rise in core body temperature observed in WT mice with prolonged heat stress is expected given that the restraint protocol prevents normal cooling behaviors, such as spreading of saliva onto their body (Barney *et al.*, 2015). Overall, the mean latency for MHS mice to trigger was not statistically different whether they received vehicle or CP and there was no genotype effect on time to trigger (Figure 7D). Kaplan-Meier curves indicated CP exposure did not decrease latency for MHS mice to trigger a fulminant MH episode (Figure 7E). All WT mice, regardless of treatment, survived the entire 60 min bought of heat stress (Figure 7E).

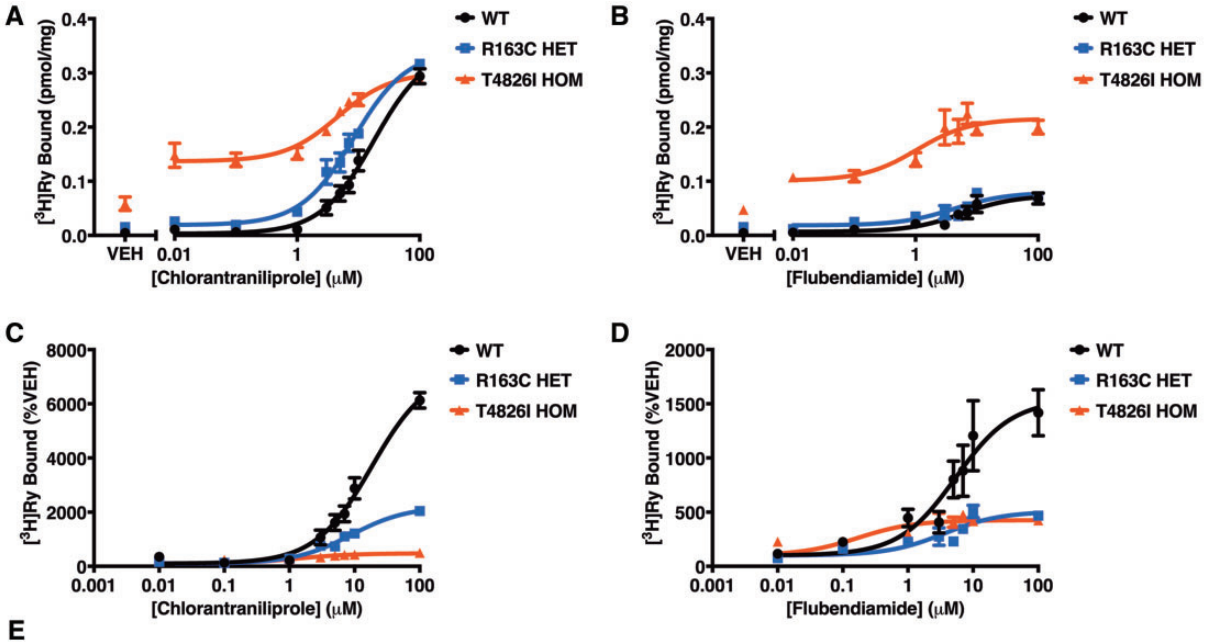

E

[Free Ca^{2+}]	Compound	Genotype	[³H]Ry Bound (pmol/mg) VEH.	Min.	Max.	Range	EC_{50} (μM) [95% C.I.]	Max. Response (%) ± SEM	LOEC# (μM)
1 μM	Chlorantraniliprole	WT	0.005	0.01	0.30	0.29	17.9 [13.1-25.6][a]	6483±450.4[a]	3
		R163C HET	0.02	0.03	0.32	0.29	8.4 [6.3-11.3]	2194±155.6[a]	3
		T4826I HOM	0.06[a]	0.15	0.29	0.14	4.6 [2.7-7.6]	491±20.5[a]	0.01
	Flubendiamide	WT	0.005	0.01	0.07	0.06	5.8 [2.0-15.2]	1538±201.3[a]	7
		R163C HET	0.02	0.02	0.08	0.06	4.2 [1.4-9.5]	506.2±48.5	7
		T4826I HOM	0.05[a]	0.10	0.22	0.12	1.1 [0.3-3.0]	425.7±19.9	0.01

(LOEC: Lowest Observed Effect Concentration)
[a]Significantly different from all other genotypes

Figure 4. At suboptimal free Ca^{2+} (1 μM), CP is more efficacious than FD with RyR1-WT and RyR1-R163C preparations, but shares similar efficacy with RyR1-T4826I preparations. Concentration-response binding of (A, C) CP or (B, D) FD at an activating concentration of Ca^{2+} expressed as either (A, B) pmol of [³H]Ry bound per mg of protein or (C, D) percent vehicle. Specific [³H]Ry binding to RyR1-WT (circle trace), heterozygous RyR1-R163C (square trace), and homozygous RyR1-T4826I (triangle trace) shown as mean ± SEM. (E) Summary for parts A–D. EC_{50} values and maximum response were analyzed using a one-way ANOVA with Tukey *post hoc* test. LOEC was analyzed using a one-way ANOVA with Dunett's *post hoc* test.

The ability of mice to thermoregulate is enhanced during short-term heat stress and as homeotherms, their initial adaptive response is to increase core body temperature (Gordon, 2012; Leon *et al.*, 2005). Interestingly, while mice typically exhibit 3 stages of thermoregulation during prolonged heat exposure—initial increase in core temperature, followed by a plateau, and finally a second more rapid increase in core temperature before succumbing to death (Wright, 1976)—R163C HET and T4826I HOM mice did not exhibit a plateau stage. Rather, MHS mice exhibited a biphasic increase in core temperature, a response to heat stress not observed with WT mice (Figs. 8A and 8B); WT mice only exhibited the initial stage of thermoregulation, which was similar between vehicle and CP exposed groups (Figure 8D). Both slopes of the biphasic heat stress response were analyzed to determine whether CP affected the ability of MHS mice to thermoregulate (Figure 8C). Mean rates for the initial phase (slope 1) of core temperature increase are not statistically different across vehicle and CP exposed groups nor across MHS genotypes (Figure 8E). Moreover, phase 2 of core temperature increase (slope 2), although 2-fold higher than the initial phase, was also unaffected by CP exposure (Figure 8F).

DISCUSSION

Diamide insecticides, including CP and FD, are utilized globally to control agricultural lepidopteran pests. Their popularity is driven by their efficacy in controlling crop losses as well as a high mammalian safety margin. The latter is attributed to their unique mode of action, which confers a high degree of selectivity toward insect RyR over mammalian RyRs. While their exact binding site(s) within insect RyR has not been fully determined, there is general consensus that binding of diamides to functionally critical regions of RyR elicits Ca^{2+} leak from skeletal muscle SR, and SR depletion mediates muscle dysfunction and insecticidal activity (Cordova *et al.*, 2006). Kato and colleagues showed that FD incorporates into the C-terminus transmembrane assembly within amino acids 4111–5084, and also requires

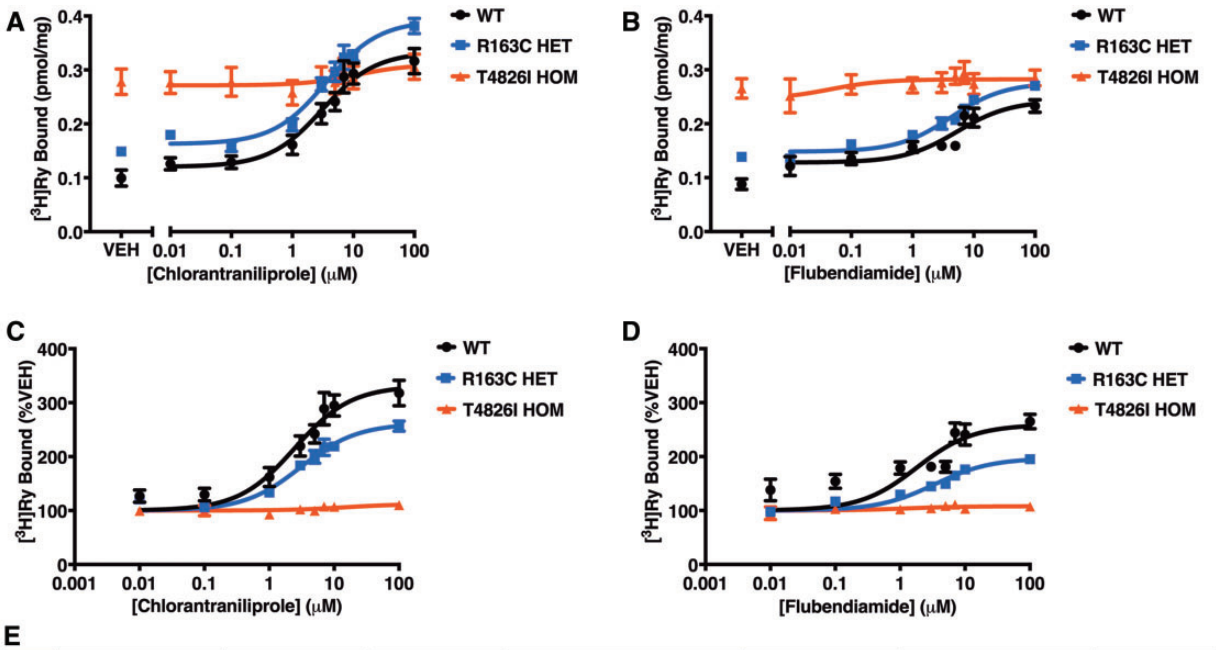

E

[Free Ca^{2+}]	Compound	Genotype	[3H]Ry Bound (pmol/mg) VEH.	Min.	Max.	Range	EC_{50} (μM) [95% C.I.]	Max. Response (%) ± SEM	LOEC# (μM)
50 μM	Chlorantraniliprole	WT	0.10	0.13	0.32	0.19	3.1 [1.5-5.8]	331.2±17.9[a]	3
		R163C HET	0.15	0.18	0.38	0.20	3.6 [2.3-5.5]	261.4±8.8[a]	3
		T4826I HOM	0.28[a]	0.28	0.31	0.03	11.3 [NA]	112.1±11.1[a]	Undetermined
	Flubendiamide	WT	0.09	0.12	0.24	0.12	5.3 [2.0-12.4]	259.2±15.0[a]	1
		R163C HET	0.14	0.14	0.28	0.14	4.3 [2.6-6.6]	197.2±5.5[a]	1
		T4826I HOM	0.27[a]	0.25	0.28	0.03	0.05 [NA]	107.9±5.5[a]	Undetermined

(LOEC: Lowest Observed Effect Concentration)
[a]Significantly different from all other genotypes

Figure 5. Optimal free Ca^{2+} (50 μM) completely saturates RyR1-T4826I preparations, but CP and FD are still able to increase [^{3}H]ryanodine ([^{3}H]Ry) binding in a concentration-dependent fashion in RyR1-WT and RyR1-R163C preparations. Concentration-response effect of (A, C) CP and (B, D) FD on specific [^{3}H]Ry binding to WT-RyR1 vesicles (circle trace), heterozygous RyR1-R163C vesicles (square trace), or homozygous RyR1-T4826I vesicles (triangle trace) at optimal [Ca^{2+}] expressed as either (A, B) pmol of [^{3}H]Ry bound per mg of protein or (C, D) percent vehicle. Traces are shown as mean ± SEM and summarized in part (E). Statistical significance with respect to EC_{50} values and maximum response were assessed using a one-way ANOVA with Tukey *post hoc* test. LOEC was assessed using a one-way ANOVA with Dunnett's *post hoc* test.

contributions from N-terminal residues 183–290 to elicit insect RyR activation (Kato *et al.*, 2009). Investigation of diamide insecticide-resistant pests by other laboratories have concluded that CP also engages critical residues within the C-terminus transmembrane assembly, in particular amino acids 4610–4946 (Tao *et al.*, 2013).

Relevance of CP Concentrations Toward Mammalian RyR1 *In Vitro*

Qi and Casida (2013) demonstrated that nM concentrations of CP or FD increases [^{3}H]Ry binding in target insect species but has negligible influence on mammalian RyR1 at <100 nM, thus concluding mammalian RyR1 lack binding sites for diamides. However, our current results demonstrate that μM concentrations of CP or FD can functionally interact with mammalian RyR1. In fact, our Ca^{2+} transport assay demonstrates that not only does acute exposure to 10 μM CP greatly enhance Ca^{2+} leak from JSR membrane vesicles, but it does so by selective action on RyR1. Our binding assay also reaffirm that CP or FD (0.01–100 μM) directly alter binding properties of [^{3}H]Ry to mammalian RyR1, and do so with differing efficacies and in a Ca^{2+}-dependent manner. Introduction of an MHS mutation in the critical diamide insecticide binding region, such as in the case of T4826I, further increased RyR1 sensitivity to the activating effects of CP, and to a lesser degree, FD. While the effects of CP or FD are comparable between RyR1-WT and RyR1-R163C, both insecticides show a stronger effect with RyR1-T4826I with LOEC being as low as 10 nM for enhancing the binding of [^{3}H]Ry in the presence of suboptimal Ca^{2+}.

The *in vitro* results presented here provide the first evidence that CP does, in fact, interact with adult mammalian WT RyR1 and promote microsomal (SR) Ca^{2+} leak. CP-induced SR Ca^{2+} leak occurs despite strong SERCA pump activity which works in opposition of RyR1-mediated Ca^{2+} leak; in the presence of CP, SERCA fails to reaccumulate Ca^{2+} into the SR lumen unless an RyR1 channel blocker is introduced (Figure 2A). The concentration (10 μM) used to demonstrate that CP is capable of eliciting a

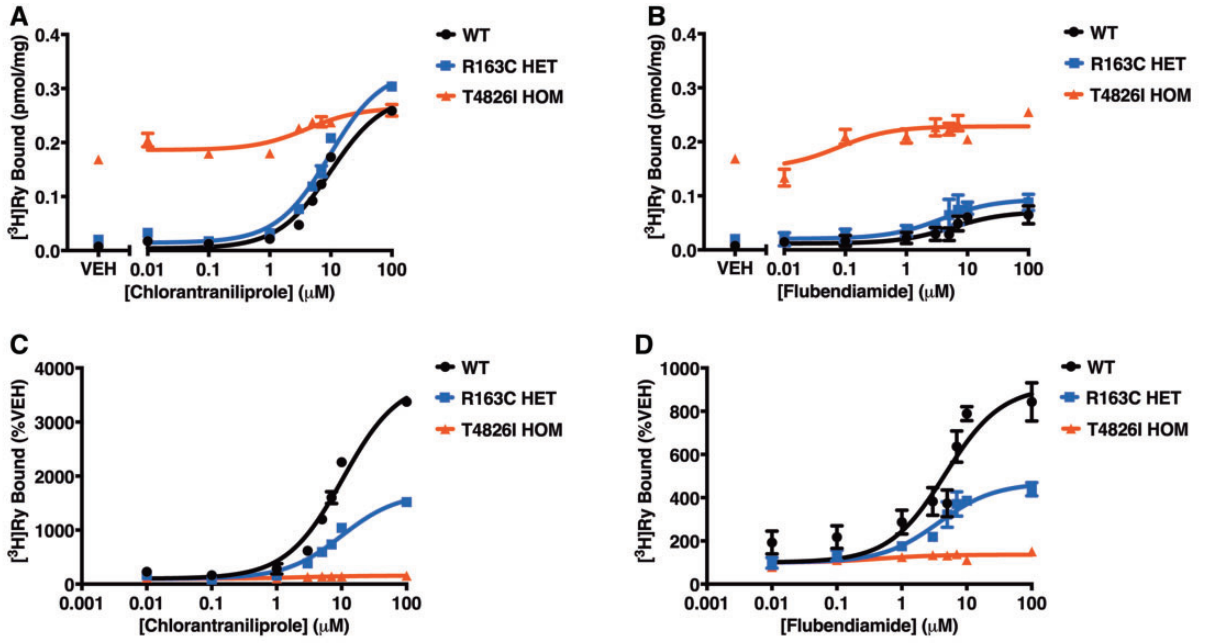

D

[Free Ca^{2+}]	Compound	Genotype	[³H]Ry Bound (pmol/mg) VEH.	Min.	Max.	Range	EC_{50} (μM) [95% C.I.]	Max. Response (%) ± SEM	LOEC# (μM)
1 mM	Chlorantraniliprole	WT	0.008	0.01	0.29	0.28	9.9 [7.9-12.6]	3792±133.9[a]	3
		R163C HET	0.02	0.02	0.34	0.32	9.5 [7.8-11.6]	1693±51.6[a]	3
		T4826I HOM	0.17[a]	0.18	0.26	0.08	4.1 [1.8-9.1]	156±5.4[a]	3
	Flubendiamide	WT	0.008	0.02	0.07	0.05	5.5 [3.0-9.6]	915.7±71.1[a]	3
		R163C HET	0.02	0.03	0.09	0.06	3.8 [1.9-6.7]	468.4±34.1[a]	5
		T4826I HOM	0.17[a]	0.21	0.23	0.02	0.08 [0.02-0.6][a]	136.1±5.6[a]	3

(LOEC: Lowest Observed Effect Concentration)
[a]Significantly different from all other genotypes

Figure 6. CP can overcome an inhibitory concentration of free Ca^{2+} (1 mM) in all 3 genotypes, whereas FD can only do so with RyR1-WT and RyR1-R163C but not with RyR1-T4826I. Concentration-response [³H]ryanodine ([³H]Ry) binding of (A, C) CP or (B, D) FD at an inhibitory [Ca^{2+}] expressed as either (A, B) pmol of [³H]Ry bound per mg of protein or (C, D) percent vehicle with RyR1-WT vesicles (circle trace), heterozygous RyR1-R163C vesicles (square trace), or homozygous RyR1-T4826I vesicles (triangle trace) plotted as mean ± SEM. (E) Summary of all 4 graphs. Statistical significance with respect to EC_{50} values and maximum response were assessed using a one-way ANOVA with Tukey *post hoc* test. LOEC was assessed using a one-way ANOVA with Dunnett's *post hoc* test.

65-fold increase over background RyR1-dependent Ca^{2+} efflux from WT mammalian SR is, in fact, comparable to the EC_{50} value (14 μM) reported for CP toward mobilizing Ca^{2+} from RyR1-expressing C2C12 embryonic muscle cells (myotubes) (Lahm *et al.*, 2009). Although CP and FD have been suggested to share insecticidal mechanisms mediated by interactions at overlapping regions within the C-terminal transmembrane domains of insect RyR, our studies indicate that FD is much less efficacious toward sensitizing mammalian RyR1 channels, suggestive of a more stringent structural requirement among diamides, consistent with previous results (Qi and Casida, 2013).

The relative potency of CP toward mammalian WT RyR1 and insect RyR (Isaacs *et al.*, 2012) measured by [³H]Ry binding analyses indicates ~200–1200-fold selectivity ratio whose magnitude is highly dependent on cytoplasmic [Ca^{2+}] as demonstrated in the present study (eg, EC_{50} = 18 μM at 1 μM Ca^{2+} vs 3 μM at 50 μM Ca^{2+}). RyR1 is highly regulated by the dynamic and large changes in cytoplasmic [Ca^{2+}] that occur during contraction-relaxation cycles in skeletal muscle, and it appears that CP (and to a lesser degree, FD) could influence contractility in a state-dependent manner. Nevertheless, the calculated LOEC for CP at mammalian WT RyR1 is 3 μM; ~200-fold higher than its S_{2x} (15 nM)—the concentration required to stimulate binding by 2-fold—reported with preparations from housefly (Isaacs *et al.*, 2012).

The activity toward adult mammalian RyR1 identified here compelled investigations into whether RyR1 channels possessing a human MHS mutation, residing within either the N- or C-terminal regions suggested to engage diamide insecticides, are differentially responsive. In fact, skeletal muscle SR preparations from T4826I homozygous mice have a 300-fold lower LOEC compared with WT or R163C heterozygous mice when tested with assay conditions that promote closure of the channel (1 μM Ca^{2+}), conditions that would exacerbate Ca^{2+} leak and augment chronically elevated cytoplasmic Ca^{2+} known to occur in skeletal muscle cells expressing MHS mutations (Feng *et al.*, 2011; Yuen *et al.*, 2012). Thus, from a mechanistic perspective, these results show that CP is capable of directly interacting with

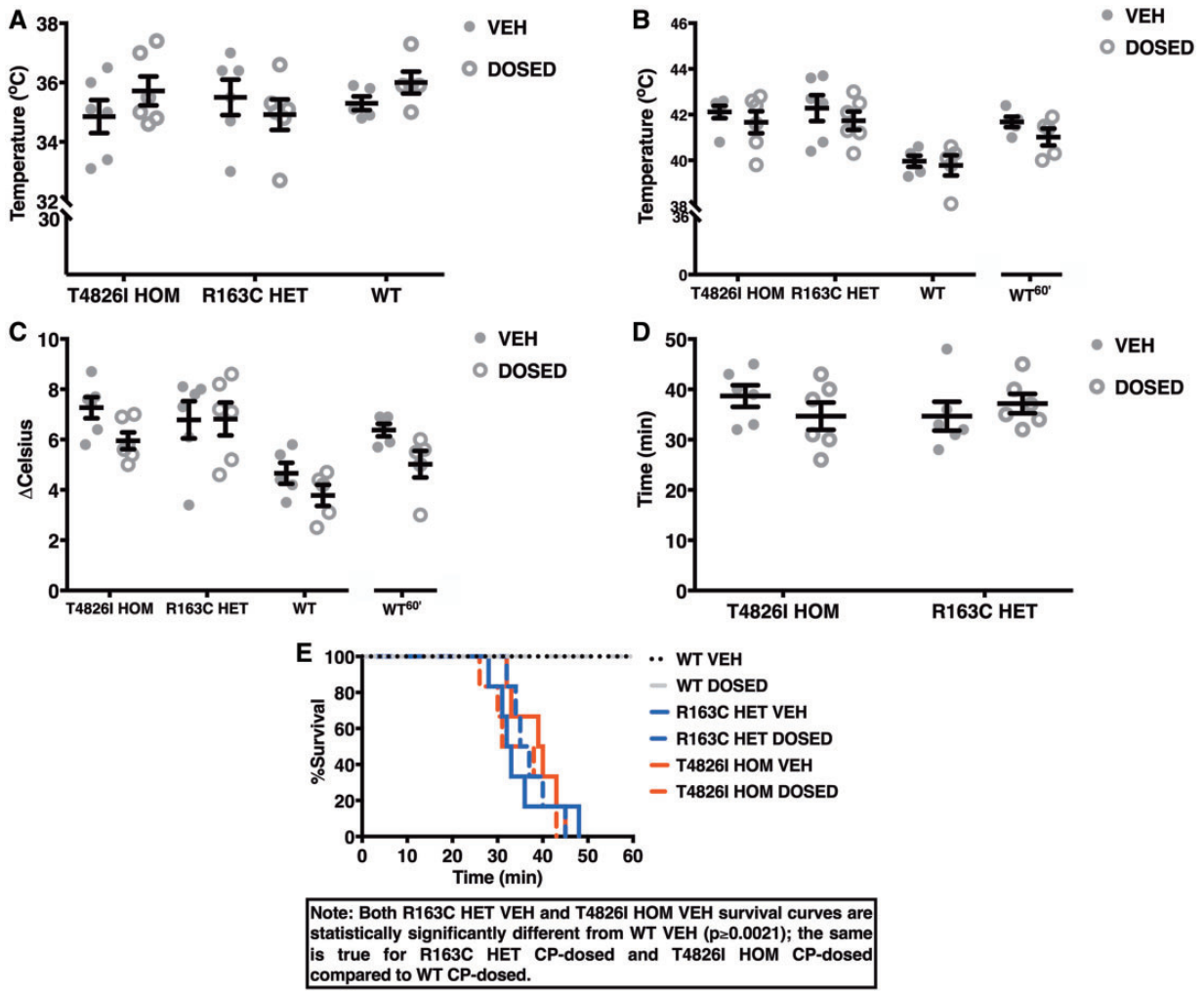

Figure 7. A 60 min heat stress study was performed and body temperature and probability of death for T4826I homozygous mice ($n = 6$), R163C heterozygous mice ($n = 6$), and WT mice ($n = 5$) were assessed. Mice were dosed with either 0.5% aqueous methyl cellulose vehicle control or 500 mg/kg bw CP and (A) initial body temperature, (B) final body temperature, and (C) the rate (°C/min) by which core body temperature increased over the course of the heat stress were analyzed. Body temperature of triggered MHS mice were compared with the body temperature of WT mice at 2 time points: (1) at the time when MHS mice triggered ($p \leq .01$) and (2) at the end of the 60' heat stress study ($WT^{60'}$). Prolonged exposure to 38°C triggered fulminant episodes in mice with a malignant hypothermia susceptible (MHS)-mutation (R163C HET and T4826I HOM), thus (D) the time required for these mice treated with vehicle control or CP was assessed. A Student's *t*-test was used to determine statistical significance between vehicle-treated and CP-treated groups. A one-way ANOVA with Tukey *post hoc* test was employed to determine statistical significance between the different genotypes. (E) A Kaplan-Meier curve (Mantel-Cox analysis) was used to determine probability of death with increasing time for T4826I HOM mice, R163C HET mice, and WT mice. Solid lines depict vehicle control and broken lines depict dosed animals. Plots shown as mean ± SEM with measurement for each individual mouse depicted as either a closed gray circle (vehicle control) or an open gray circle (CP-exposed).

RyR1-T4826I channel binding sites in a state-dependent manner at concentrations comparable to binding parameters reported with insect RyR preparations (S_{2x} of 15 nM) (Isaacs *et al.*, 2012). Based on the available data, it is reasonable to conclude that CP (and to a lesser degree FD) is not absolutely specific for insect RyR, as suggested previously (Qi and Casida, 2013). It is important that future studies investigate whether RyR1 mutations and variants associated with muscle disease in humans (Kushnir *et al.*, 2018) possess increased binding affinities for the ever-increasing diamide insecticide structures being evaluated for broader agricultural uses (Liu *et al.*, 2018; Zhou *et al.*, 2018b), and how their ability to promote SR Ca^{2+} leak influences skeletal muscle EC coupling or long-term muscle health.

Since an RyR1 channel is composed of a homotetramer, zygosity would be expected to have a significant impact upon the degree of inherent dysfunction measurable at all levels from single channel gating properties, to responses of muscle cells, to shifts in responses to physiological or xenobiotic modulator, as we have previously demonstrated (Cherednichenko *et al.*, 2008; Feng *et al.*, 2011; Ta and Pessah, 2007; Yuen *et al.*, 2012). In regards to our [^{3}H]Ry binding assay results, the T4826I homozygous genotype, where all 4 subunits carry the mutation, exhibits lower EC_{50} values (higher potency) for both CP and FD when measured in the presence of inhibitory [Ca^{2+}] (1 μM or 1 mM) compared with either WT or R163C heterozygous genotypes. However, since the T4826I mutation lies within the critical binding region for both CP and FD, we cannot discount that in addition to the inherent dysfunction contributed by the T4826I mutation, the mutation location also influences binding interactions with CP or FD. A safer conclusion, given the data, is that the greater sensitivity observed with the T4826I homozygous genotype is likely the result of a combination of both zygosity and the location of the mutation within the critical diamide binding site.

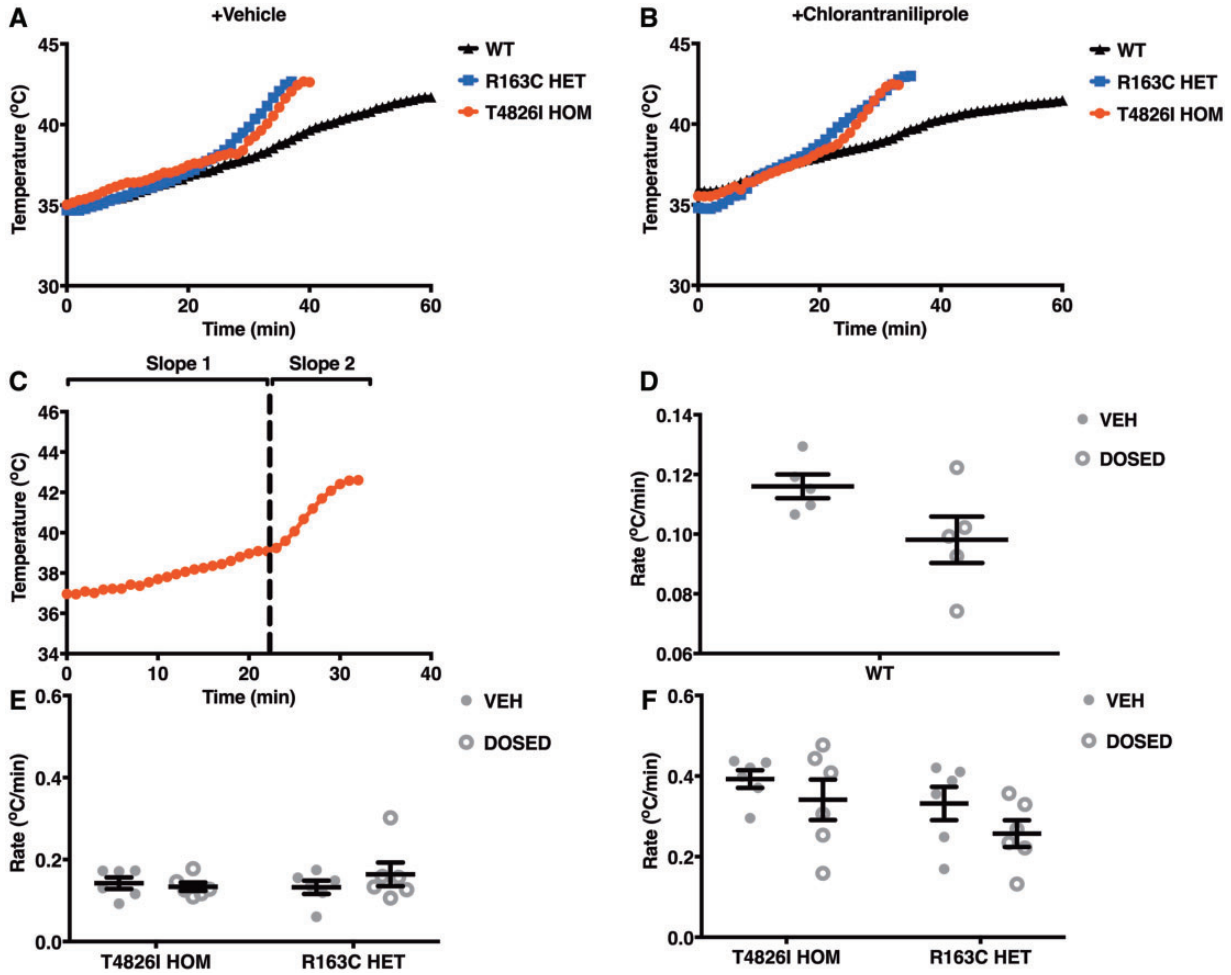

Figure 8. Regardless of whether the mice were dosed with (A) 0.5% methyl cellulose vehicle control or with (B) 500 mg/kg bw CP, WT mice (triangle trace; $n = 5$) exhibit one constant increase in body temperature, whereas R163C HET mice (square trace; $n = 6$) and T4826I HOM mice (circle trace; $n = 6$) exhibit a biphasic increase in body temperature during short-term heat stress at 38°C. (C) To determine whether CP affected the initial rate of core temperature increase or the latter rate (°C/min), both slopes were assessed with a Student's *t*-test to determine statistical significance between vehicle-treated and CP-treated groups, or a one-way ANOVA with Tukey *post hoc* test to compare between the different genotypes. (D) The sole slope of WT mice was quantified and analyzed separately with a Student *t*-test since it could not be classified as either (E) slope 1 or (F) slope 2. Plots shown as mean ± SEM with measurement for each individual mouse depicted as either a closed gray circle (vehicle control) or an open gray circle (CP exposed).

Relevance and Rationale of Acute CP Dose to Assess Influence of CP on HSI

Environmental heat stress is known to trigger fulminant episodes in MHS knock-in mice, but thought to be a less common trigger in MHS-humans who are believed to be more sensitive to inhalation anesthetics (Rosenberg 2016). HSI in MHS mice causes rapid increase in body temperature, progressive skeletal muscle rigidity, increased heart rate, and rigor mortis (Chelu *et al.*, 2006; Yang *et al.*, 2006; Yuen *et al.*, 2012). A similar event is observed in HSI MHS humans: skeletal and jaw muscle rigidity, tachycardia, fever, and occasionally fatality (Gronert *et al.*, 2011). HSI is less understood in MHS humans due to the paucity of reported cases. The number of HSI MHS individuals may be underestimated due to miscategorization as death by exertional heat stroke (EHS). Figarella-Branger and colleagues investigated 45 patients diagnosed as succumbing to EHS, but *in vitro* contracture testing confirmed most were MHS positive (Figarella-Branger *et al.*, 1993). Sagui investigated 466 EHS subjects who suffered from muscle abnormalities and an increase in body temperature and determined that half were MHS positive (Sagui *et al.*, 2015). These studies demonstrate how often MH episodes are misdiagnosed as EHS, and that exposure to nonanesthetic triggers do not always cause lethality but can lead to weakness. Our study, therefore, investigated the important question of whether a second nonanesthetic stress factor like CP can shift HSI to cause earlier onset of MH episodes.

Our restraint HSI model enabled continuous digital measurement of mouse core body temperature across genotype and dose groups as they experienced moderate heat stress—a protocol not previously investigated with these MHS lines. A new observation is that these genotypes exhibit a thermoregulation pattern that may be unique to MHS mice: they have a biphasic response to temperature stress, whereas WT mice exhibit a monotonic core temperature response. Although significant biochemical difference was observed in the ability of CP to alter SR Ca^{2+} leak and [^{3}H]Ry binding parameters, especially with T4826I homozygous preparations, such differences do not appear to be sufficient to cause detectable shifts in HSI response, at least using the acute heat stress exposure protocol investigated here. The reason for the lack of an anticipated rightward shift in HSI with respect to changes in core body temperature

and latency in triggering fulminant MH episode is unlikely due to CP not attaining sufficient concentrations at its target in skeletal muscle. The high-dose protocol used in the present study is based on available pharmacokinetic literature for oral exposure which would be expected to reach a C_{max} of 5.1 μg/g plasma (11 μM) at 12 h (FAO/WHO, 2008). Considering that skeletal muscles are highly perfused, a peak concentration in the μM range would be anticipated at the time mice were tested for HSI, although direct measurements in the skeletal muscle compartment are unfound in the accessible literature. However, a detectable fraction of the CP oral dose is detected in tissues 48 h (3%) and 168 h (0.2%) post-administration (FAO/WHO, 2008). While the lack of detectable influences of CP on HSI and thermoregulation with T486I HOM and R163C HET mice is unlikely the results of insufficient levels reaching skeletal muscle, we cannot discount that the high dosing protocol failed to distribute CP across the basement membranes and into the myoplasm in sufficient concentrations to influence RyR1 mediated signaling.

Although the present study provides strong evidence that mammalian RyR1 recognizes 2 of the rapidly growing number of insecticidal diamides intended for broader spectrum agricultural uses (Liu *et al.*, 2018; Zhou *et al.*, 2018b), the acute high-dose HSI protocol used here does not have the sensitivity to unmask an anticipated gene by environment interaction predicted by *in vitro* studies. One likely complication in directly translating measures of RyR1 dysfunction *in vitro* to detecting abnormal acute responses *in vivo* is the possible loss of the highly regulated nature of RyR1 channels by a large number of protein-protein associations during SR membrane isolation and purification. The most important and relevant of these interactions is with the L-type Ca^{2+} channel (Cav1.1) that forms a conformationally coupled unit with RyR1. It not only confers physical activation of RyR1 triggered by conformational changes during transverse tubules depolarization, but it also has very strong orthograde regulation that suppresses RyR1 channel activity and Ca^{2+} leak at rest in context of the intact skeletal muscle triad (Bannister *et al.*, 2009; Eltit *et al.*, 2011). Cav1.1-RyR1 interactions have been suggested to mask potentially devastating unregulated SR Ca^{2+} leak in muscle that expresses RyR1 channel mutations; although, clearly, this critical form of negative regulation is weakened by the presence of these mutations possibly contributing to increased susceptibility to environmental and chemical stressors (Barrientos *et al.*, 2012; Eltit *et al.*, 2011; Yuen *et al.*, 2012). Regardless, it is important to emphasize that the limited acute HSI test investigated here may have missed important gene by environment interactions *in vivo*, since an increasing number of expressed mutations and genetic variants identified in humans are being associated with skeletal muscle disease and myopathies (Kushnir *et al.*, 2018). Changes in RyR1 regulation and conformation make the Ca^{2+} channel more sensitive to allosteric modulation by pharmacological and environmental factors, including heat stress (Mackrill 2010; Pessah *et al.*, 2010). It is important that future safety studies address whether long-term chronic exposures influence physiological and/or myopathic outcomes known to be mediated by RyR1 dysfunction, especially in populations expressing mutations known to affect muscle health. The present study investigated only 2 of 34 mutations within RyR1 demonstrated to confer MHS in humans and known to influence responses to potentially lethal environmental triggers, although an additional 400 *RYR1* mutations have been identified in the human genome, to date, of which we have little understanding regarding their influences on long-term muscle health (Rosenberg *et al.*, 2015; Zhou *et al.*, 2018a).

MHS RyR1 mutations do not always lead to fatal episodes—they can confer subtler chronic myopathies like rhabdomyolysis and exertional myalgia (Dlamini *et al.*, 2013; Voermans *et al.*, 2016). The current results show that while CP and FD at concentrations higher than those needed to modify the function of lepidopteran RyR influence [^{3}H]Ry binding to mammalian WT RyR1, MHS mutations lower the LOEC for these effects in a Ca^{2+}-dependent (state-dependent) manner. Whether any of the 400+ MHS mutations confer risk to skeletal muscle health with prolonged CP exposure remains a difficult question to address. Although there are numerous documented cases of MHS individuals who experienced nonfatal episodes and spontaneously developed muscle weakness or rhabdomyolysis following exposure to environmental stressor(s) (Dlamini *et al.*, 2013; Thomas and Crowhurst 2013), whether CP, FD, or other insecticide diamides interact with MHS RyR1 channels to lower the threshold for developing chronic myopathies remains unknown.

Currently, numerous point mutations have been identified within Lepidopteran RyR that confer a high degree of resistance (200- to >1000-fold) to diamide insecticides (Roditakis *et al.*, 2017; Troczka *et al.*, 2012; 2017). Increased resistance will have strong implications regarding pest management strategies, making the use of a higher concentration of CP inevitable. Ultimately, future studies are needed to investigate whether chronic exposures to insecticidal diamides under well-established exercise and heat stress protocols differentially influence the onset and progression of muscle injury in MHS mice that genocopy and phenocopy those found in humans.

ACKNOWLEDGMENTS

Dedicated to Professor John E. Casida. We thank Dr Wei Feng for his thorough review of the manuscript and helpful suggestions.

FUNDING

This work was supported by the National Institute of Environmental Health Sciences (R01 ES014901, P01 AR052354, P01 ES011269, and P42 ES04699) and the U.S. Environmental Protection Agency (STARR829388 and R833292).

REFERENCES

Adams, A., Gore, J., Catchot, A., Musser, F., Cook, D., Krishnan, N., and Irby, T. (2016). Residual and systemic efficacy of chlorantraniliprole and flubendiamide against corn earworm (Lepidoptera: Noctuidae) in Soybean. *J. Econ. Entomol.* **109**, 2411–2417.

Bannister, R. A., Pessah, I. N., and Beam, K. G. (2009). The skeletal L-type Ca(2+) current is a major contributor to excitation-coupled Ca(2+) entry. *J. Gen. Physiol.* **133**, 79–91.

Barney, C. C., Schanhals, E. M., Grobe, J. L., Andresen, B. T., and Traver, M. (2015). Heat acclimation and thirst in rats. *Physiol. Rep.* **3(12)**, e12642.

Barrientos, G. C., Feng, W., Truong, K., Matthaei, K. I., Yang, T., Allen, P. D., Lopez, J. R., and Pessah, I. N. (2012). Gene dose influences cellular and calcium channel dysregulation in heterozygous and homozygous T4826I-RYR1 malignant hyperthermia-susceptible muscle. *J. Biol. Chem.* **287**, 2863–2876.

Bentley, K. S., Fletcher, J. L., and Woodward, M. D. (2010a) *Chapter 102—Chlorantraniliprole: An Insecticide of the Anthranilic Diamide Class A2—Krieger, Robert Hayes' Handbook of Pesticide Toxicology*, 3rd ed., pp. 2231–2242. Academic Press, New York.

Bentley, K. S., Fletcher, J. L., and Woodward, M. D. (2010b) Chlorantraniliprole: An insecticide of the anthranilic diamide class. In *Hayes' Handbook of Pesticide Toxicology* (R Krieger, Ed.), 3rd ed., pp. 2231–2242. Academic Press, New York.

Brooks, S. P., and Storey, K. B. (1992). Bound and determined: A computer program for making buffers of defined ion concentrations. *Anal. Biochem.* **201**, 119–126.

Cameron, R. A., Williams, C. J., Portillo, H. E., Marçon, P. C., and Teixeira, L. A. (2015). Systemic application of chlorantraniliprole to cabbage transplants for control of foliar-feeding lepidopteran pests. *Crop Protect.* **67**, 13–19.

Casida, J. E. (2015). Golden age of RyR and GABA-R diamide and isoxazoline insecticides: Common genesis, serendipity, surprises, selectivity, and safety. *Chem. Res. Toxicol.* **28**, 560–566.

Chelu, M. G., Goonasekera, S. A., Durham, W. J., Tang, W., Lueck, J. D., Riehl, J., Pessah, I. N., Zhang, P., Bhattacharjee, M. B., Dirksen, R. T., *et al.* (2006). Heat- and anesthesia-induced malignant hyperthermia in an RyR1 knock-in mouse. *FASEB J.* **20**, 329–330.

Cherednichenko, G., Ward, C. W., Feng, W., Cabrales, E., Michaelson, L., Samso, M., Lopez, J. R., Allen, P. D., and Pessah, I. N. (2008). Enhanced excitation-coupled calcium entry in myotubes expressing malignant hyperthermia mutation R163C is attenuated by dantrolene. *Mol. Pharmacol.* **73**, 1203–1212.

Cordova, D., Benner, E. A., Sacher, M. D., Rauh, J. J., Sopa, J. S., Lahm, G. P., Selby, T. P., Stevenson, T. M., Flexner, L., Gutteridge, S., *et al.* (2006). Anthranilic diamides: A new class of insecticides with a novel mode of action, ryanodine receptor activation. *Pestic. Biochem. Physiol.* **84**, 196–214.

Dlamini, N., Voermans, N. C., Lillis, S., Stewart, K., Kamsteeg, E.-J., Drost, G., Quinlivan, R., Snoeck, M., Norwood, F., Radunovic, A., *et al.* (2013). Mutations in RYR1 are a common cause of exertional myalgia and rhabdomyolysis. *Neuromuscul. Disord.* **23**, 540–548.

Dulhunty, A. F., Wei-LaPierre, L., Casarotto, M. G., and Beard, N. A. (2017). Core skeletal muscle ryanodine receptor calcium release complex. *Clin. Exp. Pharmacol. Physiol.* **44**, 3–12.

Eltit, J. M., Li, H., Ward, C. W., Molinski, T., Pessah, I. N., Allen, P. D., and Lopez, J. R. (2011). Orthograde dihydropyridine receptor signal regulates ryanodine receptor passive leak. *Proc. Natl. Acad. Sci. U.S.A.* **108**, 7046–7051.

EPA. (2018) Flubendiamide—Notice of Intent to Cancel and Other Supporting Documents. https://www.epa.gov/ingredients-used-pesticide-products/flubendiamide-notice-intent-cancel-and-other-supporting Access May 30, 2018.

Fagerlund, T. H., Islander, G., Ranklev Twetman, E., and Berg, K. (1997). Malignant hyperthermia susceptibility, an autosomal dominant disorder? *Clin. Genet.* **51**, 365–369.

FAO/WHO (2008) Pesticide residues in food - 2008 Part II toxicological evaluations: Chlorantraniliprole. In FAO/WHO (ed), p. 106. Switzerland: World Health Organization.

Feng, W., Barrientos, G. C., Cherednichenko, G., Yang, T., Padilla, I. T., Truong, K., Allen, P. D., Lopez, J. R., and Pessah, I. N. (2011). Functional and biochemical properties of ryanodine receptor type 1 channels from heterozygous R163C malignant hyperthermia-susceptible mice. *Mol. Pharmacol.* **79**, 420–431.

Feng, W., Zheng, J., Robin, G., Dong, Y., Ichikawa, M., Inoue, Y., Mori, T., Nakano, T., and Pessah, I. N. (2017). Enantioselectivity of 2, 2', 3, 5', 6-pentachlorobiphenyl (PCB 95) atropisomers toward ryanodine receptors (RyRs) and their influences on hippocampal neuronal networks. *Environ. Sci. Technol.* **51**, 14406–14416.

Figarella-Branger, D., Kozak-Ribbens, G., Rodet, L., Aubert, M., Borsarelli, J., Cozzone, P.J., and Pellissier, J.F. (1993). Pathological findings in 165 patients explored for malignant hyperthermia susceptibility. *Neuromuscul. Disord.* **3**, 553–556.

Gordon, C. J. (2012). The mouse: An "average" homeotherm. *J. Therm. Biol.* **37**, 286–290.

Gronert, G. A., Tobin, J. R., and Muldoon, S. (2011). Malignant hyperthermia: Human stress triggering. *Biochim. Biophys. Acta* **1813**, 2191–2192; author reply 2193–4.

Hawkes, M. J., Nelson, T. E., and Hamilton, S. L. (1992). [3H]ryanodine as a probe of changes in the functional state of the Ca(2+)-release channel in malignant hyperthermia. *J. Biol. Chem.* **267**, 6702–6709.

Himmelstein, M. W. (2006a) *14C-DPX-E2Y45: Absorption, Distribution, Metabolism and Excretion in Male and Female Rats*. DuPont Haskell Laboratory. E.I. du Pont de Nemours and Company, Newark, DE.

Isaacs, A. K., Qi, S., Sarpong, R., and Casida, J. E. (2012). Insect ryanodine receptor: Distinct but coupled insecticide binding sites for [N-C(3)H(3)]chlorantraniliprole, flubendiamide, and [(3)H]ryanodine. *Chem. Res. Toxicol.* **25**, 1571–1573.

Kato, K., Kiyonaka, S., Sawaguchi, Y., Tohnishi, M., Masaki, T., Yasokawa, N., Mizuno, Y., Mori, E., Inoue, K., Hamachi, I., *et al.* (2009). Molecular characterization of flubendiamide sensitivity in the lepidopterous ryanodine receptor Ca(2+) release channel. *Biochemistry* **48**, 10342–10352.

Kim, D. C. (2012). Malignant hyperthermia. *Korean J. Anesthesiol.* **63**, 391–401. CrossRef][10.4097/kjae.2012.63.5.391]

Kushnir, A., Wajsberg, B., and Marks, A. R. (2018) Ryanodine receptor dysfunction in human disorders. *Biochim. Biophys. Acta* doi:10.1016/j.bbamcr.2018.07.011.

Lahm, G. P., Cordova, D., and Barry, J. D. (2009). New and selective ryanodine receptor activators for insect control. *Bioorg. Med. Chem.* **17**, 4127–4133.

Leon, L. R., DuBose, D. A., and Mason, C. W. (2005). Heat stress induces a biphasic thermoregulatory response in mice. *Am. J. Physiol. Regul. Integr. Comp. Physiol.* **288**, R197–R204.

Liu, J.-B., Li, F.-Y., Dong, J.-Y., Li, Y.-X., Zhang, X.-L., Wang, Y.-H., Xiong, L.-X., and Li, Z.-M. (2018). Anthranilic diamides derivatives as potential ryanodine receptor modulators: Synthesis, biological evaluation and structure activity relationship. *Bioorg. Med. Chem.* **26**, 3541–3550.

Lyfenko, A. D., Goonasekera, S. A., and Dirksen, R. T. (2004). Dynamic alterations in myoplasmic Ca2+ in malignant hyperthermia and central core disease. *Biochem. Biophys. Res. Commun.* **322**, 1256–1266.

Ma, J., Fill, M., Knudson, C. M., Campbell, K. P., and Coronado, R. (1988). Ryanodine receptor of skeletal muscle is a gap junction-type channel. *Science* **242**, 99–102.

Mackrill, J. J. (2010). Ryanodine receptor calcium channels and their partners as drug targets. *Biochem. Pharmacol.* **79**, 1535–1543.

Meissner, G. (1994). Ryanodine receptor/Ca2+ release channels and their regulation by endogenous effectors. *Annu. Rev. Physiol.* **56**, 485–508.

Meissner, G. (2017). The structural basis of ryanodine receptor ion channel function. *J. Gen. Physiol.* **149**, 1065–1089.

Niknam, Y., Feng, W., Cherednichenko, G., Dong, Y., Joshi, S. N., Vyas, S. M., Lehmler, H.-J., and Pessah, I. N. (2013). Structure-activity relationship of selected meta- and para-hydroxylated non-dioxin like polychlorinated biphenyls: From single RyR1 channels to muscle dysfunction. *Toxicol. Sci.* **136**, 500–513.

Pessah, I. N., and Zimanyi, I. (1991). Characterization of multiple [3H]ryanodine binding sites on the Ca2+ release channel of sarcoplasmic reticulum from skeletal and cardiac muscle: Evidence for a sequential mechanism in ryanodine action. *Mol. Pharmacol.* **39**, 679–689.

Pessah, I. N., Anderson, K. W., and Casida, J. E. (1986). Solubilization and separation of Ca2+-ATPase from the Ca2+-ryanodine receptor complex. *Biochem. Biophys. Res. Commun.* **139**, 235–243.

Pessah, I. N., Cherednichenko, G., and Lein, P. J. (2010). Minding the calcium store: Ryanodine receptor activation as a convergent mechanism of PCB toxicity. *Pharmacol. Ther.* **125**, 260–285.

Pessah, I. N., Hansen, L. G., Albertson, T. E., Garner, C. E., Ta, T. A., Do, Z., Kim, K. H., and Wong, P. W. (2006). Structure-activity relationship for noncoplanar polychlorinated biphenyl congeners toward the ryanodine receptor-Ca2+ channel complex type 1 (RyR1). *Chem. Res. Toxicol.* **19**, 92–101.

Pessah, I. N., Lehmler, H.-J., Robertson, L. W., Perez, C. F., Cabrales, E., Bose, D. D., and Feng, W. (2009). Enantiomeric specificity of (-)-2, 2', 3, 3', 6, 6'-hexachlorobiphenyl toward ryanodine receptor types 1 and 2. *Chem. Res. Toxicol.* **22**, 201–207.

Pessah, I. N., Stambuk, R. A., and Casida, J. E. (1987). Ca2+-activated ryanodine binding: Mechanisms of sensitivity and intensity modulation by Mg2+, caffeine, and adenine nucleotides. *Mol. Pharmacol.* **31**, 232–238.

Pessah, I. N., Waterhouse, A. L., and Casida, J. E. (1985). The calcium-ryanodine receptor complex of skeletal and cardiac muscle. *Biochem. Biophys. Res. Commun.* **128**, 449–456.

Qi, S., and Casida, J. E. (2013). Species differences in chlorantraniliprole and flubendiamide insecticide binding sites in the ryanodine receptor. *Pestic. Biochem. Physiol.* **107**, 321–326.

Riazi, S., Kraeva, N., and Hopkins, P. M. (2018). Malignant hyperthermia in the post-genomics era: New perspectives on an old concept. *Anesthesiology* **128**, 168–180.

Robinson, R., Carpenter, D., Shaw, M. A., Halsall, J., and Hopkins, P. (2006). Mutations in RYR1 in malignant hyperthermia and central core disease. *Hum. Mutat.* **27**, 977–989.

Roditakis, E., Steinbach, D., Moritz, G., Vasakis, E., Stavrakaki, M., Ilias, A., García-Vidal, L., Martínez-Aguirre, M. d R., Bielza, P., Morou, E., *et al.* (2017). Ryanodine receptor point mutations confer diamide insecticide resistance in tomato leafminer, *Tuta absoluta* (Lepidoptera: Gelechiidae). *Insect. Biochem. Mol. Biol.* **80**, 11–20.

Rosenberg, H., Davis, M., James, D., Pollock, N., and Stowell, K. (2007). Malignant hyperthermia. *Orphanet. J. Rare Dis.* **2**, 21.

Rosenberg, H., Pollock, N., Schiemann, A., Bulger, T., and Stowell, K. (2015). Malignant hyperthermia: A review. *Orphanet. J. Rare Dis.* **10**, 93.

Sagui, E., Montigon, C., Abriat, A., Jouvion, A., Duron-Martinaud, S., Canini, F., Zagnoli, F., Bendahan, D., Figarella-Branger, D., Brégigeon, M., *et al.* (2015). Is there a link between exertional heat stroke and susceptibility to malignant hyperthermia? *PLoS One* **10**, e0135496.

Saito, A., Seiler, S., Chu, A., and Fleischer, S. (1984). Preparation and morphology of sarcoplasmic reticulum terminal cisternae from rabbit skeletal muscle. *J. Cell Biol.* **99**, 875–885.

Sattelle, D. B., Cordova, D., and Cheek, T. R. (2008). Insect ryanodine receptors: Molecular targets for novel pest control chemicals. *Invert. Neurosci.* **8**, 107.

Selby, T. P., Lahm, G. P., Stevenson, T. M., Hughes, K. A., Cordova, D., Annan, I. B., Barry, J. D., Benner, E. A., Currie, M. J., Pahutski, T. F., *et al.* (2013). Discovery of cyantraniliprole, a potent and selective anthranilic diamide ryanodine receptor activator with cross-spectrum insecticidal activity. *Bioorg. Med. Chem. Lett.* **23**, 6341–6345.

Sun, L. N., Zhang, H. J., Quan, L. F., Yan, W. T., Yue, Q., Li, Y. Y., and Qiu, G. S. (2016). Characterization of the ryanodine receptor gene with a unique 3'-UTR and alternative splice site from the oriental fruit moth. *J. Insect. Sci.* **16**, 16.

Ta, T. A., and Pessah, I. N. (2007). Ryanodine receptor type 1 (RyR1) possessing malignant hyperthermia mutation R615C exhibits heightened sensitivity to dysregulation by non-coplanar 2, 2', 3, 5', 6-pentachlorobiphenyl (PCB 95). *Neurotoxicology* **28**, 770–779.

Tao, Y., Gutteridge, S., Benner, E. A., Wu, L., Rhoades, D. F., Sacher, M. D., Rivera, M. A., Desaeger, J., and Cordova, D. (2013). Identification of a critical region in the Drosophila ryanodine receptor that confers sensitivity to diamide insecticides. *Insect. Biochem. Mol. Biol.* **43**, 820–828.

Thomas, J., and Crowhurst, T. (2013). Exertional heat stroke, rhabdomyolysis and susceptibility to malignant hyperthermia. *Intern. Med. J.* **43**, 1035–1038.

Troczka, B. J., Williamson, M. S., Field, L. M., and Davies, T. G. E. (2017). Rapid selection for resistance to diamide insecticides in *Plutella xylostella* via specific amino acid polymorphisms in the ryanodine receptor. *Neurotoxicology* **60**, 224–233.

Troczka, B., Zimmer, C. T., Elias, J., Schorn, C., Bass, C., Davies, T. G. E., Field, L. M., Williamson, M. S., Slater, R., Nauen, R., *et al.* (2012). Resistance to diamide insecticides in diamondback moth, *Plutella xylostella* (Lepidoptera: Plutellidae) is associated with a mutation in the membrane-spanning domain of the ryanodine receptor. *Insect. Biochem. Mol. Biol.* **42**, 873–880.

Voermans, N. C., Snoeck, M., and Jungbluth, H. (2016). RYR1-related rhabdomyolysis: A common but probably underdiagnosed manifestation of skeletal muscle ryanodine receptor dysfunction. *Rev. Neurol.* **172**, 546–558.

Wappler, F. (2010). Anesthesia for patients with a history of malignant hyperthermia. *Curr. Opin. Anaesthesiol.* **23**, 417–422.

Wolterink, G.and Dellarco, V. (2008). Chlorantraniliprole, First draft, Joint FAO/WHO Meeting on Pesticide Residues (JMPR), 2008, pp. 105–134.

Wright, G. L. (1976). Critical thermal maximum in mice. *J. Appl. Physiol.* **40**, 683–687.

Xu, X., Bhat, M. B., Nishi, M., Takeshima, H., and Ma, J. (2000). Molecular cloning of cDNA encoding a drosophila ryanodine receptor and functional studies of the carboxyl-terminal calcium release channel. *Biophys. J.* **78**, 1270–1281.

Yamada, T., Steinz, M. M., Kenne, E., and Lanner, J. T. (2017). Muscle weakness in rheumatoid arthritis: The role of Ca(2+) and free radical signaling. *EBioMedicine* **23**, 12–19.

Yang, T., Riehl, J., Esteve, E., Matthaei, K. I., Goth, S., Allen, P. D., Pessah, I. N., and Lopez, J. R. (2006). Pharmacologic and functional characterization of malignant hyperthermia in the R163C RyR1 knock-in mouse. *Anesthesiology* **105**, 1164–1175.

Yuen, B., Boncompagni, S., Feng, W., Yang, T., Lopez, J. R., Matthaei, K. I., Goth, S. R., Protasi, F., Franzini-Armstrong, C., Allen, P. D., *et al.* (2012). Mice expressing T4826I-RYR1 are viable but exhibit sex- and genotype-dependent susceptibility

to malignant hyperthermia and muscle damage. *Faseb J.* **26**, 1311–1322.

Zhang, R., and Pessah, I. N. (2017). Divergent mechanisms leading to signaling dysfunction in embryonic muscle by bisphenol A and tetrabromobisphenol A. *Mol. Pharmacol.* **91**, 428–436.

Zhou, J., Nozari, A., Bateman, B., Allen, P. D., and Pessah, I. N. (2018a) *Malignant Hyperthermia and Other Related Disorders* *Miller's Anesthesia*, 9th ed. Elsevier Health Sciences, New York.

Zhou, Y., Wei, W., Zhu, L., Li, Y., and Li, Z. (2018b) Synthesis and insecticidal activity study of novel anthranilic diamides analogs containing a diacylhydrazine bridge as effective Ca(2+) modulators. *Chem. Biol. Drug Des.* doi:10.1111/cbdd.13349.